Perturbative numeric approach in microwave imaging

Anna Rozanova-Pierrat

Applicable Analysis
Vol. 00, No. 00, January 2008, 1–21

RESEARCH ARTICLE

Perturbative numeric approach in microwave imaging

A. Rozanova-Pierrat[a] *

[a]*Laboratoire de la Physique de la Matire Condense, cole Polytechnique, Route de Saclay, 91120 Palaiseau, France*

(*v3.3 released May 2008*)

In this paper, we show that using measurements for different frequencies, and using ultrasound localized perturbations it is possible to extend the method of the imaging by elastic deformation developed by Ammari and al. [Electrical Impedance Tomography by Elastic Deformation SIAM J. Appl. Math. , 68(6), (2008), 1557–1573.] to problems of the form

$$\begin{aligned} \operatorname{div}(\gamma\nabla u) + k^2 q u &= 0 \quad \text{in } \Omega, \\ \gamma\frac{\partial u}{\partial n} &= \varphi \quad \text{on } \partial\Omega, \end{aligned}$$

and to reconstruct by a perturbation method both γ and q, provided that γ is coercive and k is not a resonant frequency.

Keywords: imaging, Helmholtz equation, perturbations, inverse problem, asymptotic analysis

AMS Subject Classification: 31B20; 31A25

1. Introduction and Notations

In the recent years, a lot of attention has been devoted to the reconstruction of physical parameters of partial differential equations from electromagnetic measurements. In the case of electrical impedance tomography (EIT) it is well known that the detection of the conductivity from boundary measurements is a very ill-conditioned problem. This drawback has limited its use so far to anomaly detection. In a recent work, Ammari *et al.* have shown that combining these measurements with simultaneous localized ultrasonic perturbations allows to recover the conductivity with great precision. The purpose of this work is to show that such an approach can be generalized successfully to the study of Helmholtz type problems.

In what follows we use the following notations:

- Ω is a smooth domain in $\mathbb{R}^n$ with a regular boundary denoted by $\partial\Omega$,
- x is a point in Ω,
- $\Omega' = \{x \in \Omega | \operatorname{dist}(x, \partial\Omega) \geq d_0 > 0\}$ represents the interior points of Ω,
- $w \subset \Omega'$ is the region of the localization of the ultrasound perturbations, which is supposed to be small compared to the size of Ω',
- $|w|$ is the volume of w,

*Corresponding author. Email: anna.rozanova-pierrat@polytechnique.edu

ISSN: 0003-6811 print/ISSN 1563-504X online

DOI: 10.1080/0003681YYxxxxxxxx
http://www.informaworld.com

- 1_w denotes the characteristic function corresponding to the set w, i.e., the function which takes the value 1 on the set and the value 0 outside,
- $z \in w$ is the centre point of the region of the ultrasound perturbation,
- $k_i > 0$ is a frequency,
- $\gamma(x)$ is the conductivity and is a scalar real-valued function such that $0 < c_0 < \gamma(x) < C_0$ for all $x \in \overline{\Omega}$,
- $q(x)$ is the permittivity and is a scalar real-valued function such that $0 < c_0 < q(x) < C_0$ for all $x \in \overline{\Omega}$,
- $u(x)$ is the potential induced on the boundary by the electromagnetic field φ in the absence of ultrasonic perturbations ($u(x)$ and $\varphi(x)$ are complex-valued functions),
- u_w is the perturbed potential field induced on the boundary by the electromagnetic field φ in the presence of ultrasonic perturbations localized in the domain w (u_w is a complex-valued function),
- λ is the amplitude of the ultrasonic perturbation,
- $\gamma_w(x)$ is the perturbed conductivity (real-valued positive bounded function),
- $\tilde{\gamma}$ is the value of the perturbed conductivity γ_w in the area w of the perturbation (real-valued positive bounded function),
- $q_w(x)$ is the perturbed permittivity (real-valued positive bounded function),
- $\tilde{q}$ is the value of the perturbed permittivity q_w in the area w of the perturbation (real-valued positive bounded function),
- $\mathbf{M}_w$ and $\mathbf{m}_w$ are the polarization tensors,
- $N_{\gamma,q}(x,z)$ is the Neumann function for the operator $\mathrm{div}(\gamma(x)\nabla_x) + q(x)$ in Ω corresponding to a Dirac mass at z,
- $W^1_\infty(\Omega)$ is the Sobolev space of the functions $u(x)$ such that $u \in L_\infty(\Omega)$ and $\nabla u \in L_\infty(\Omega)$,
- for the complex-valued function u, the function $\overline{u}$ denotes its complex-conjugated.

The problem we consider is the following. Let $\gamma \in C^1(\Omega)$ and $q \in C^0(\Omega)$ be bounded scalar real-valued functions (see the list of notations). For $i = 1, 2$, let $u_i \in H^1(\Omega)$ be such that

$$\mathrm{div}(\gamma \nabla u_i) + k_i^2 q u_i = 0 \quad \text{in } \Omega, \tag{1}$$

$$\gamma \frac{\partial u_i}{\partial \nu} = \varphi_i \text{ on } \partial\Omega. \tag{2}$$

The well-posedness of this problem requires that k_i^2 is not an eigenvalue of the generalized eigenvalue problem

$$-\mathrm{div}(\gamma \nabla u) = \lambda q u \quad \text{in } \Omega, \tag{3}$$

$$\gamma \frac{\partial u}{\partial \nu} = 0 \quad \text{on } \partial\Omega.$$

It is well known that this problem admits a countable number of eigenmodes, with no accumulation point, and that each eigenvalue as a finite multiplicity. We will assume that k_1 and k_2 do not correspond to eigenvalues of problem (3). The generalization of the method introduced in [1] is the following. For frequency k_i being fixed, we measure the potential u_i, solution of problem (1)-(2), on $\partial\Omega$.

Assume now that ultrasonic waves are localized around a point $z \in \Omega$, creating a local change in the physical parameters of the medium. Further, we suppose that q and γ are known close to the boundary of the domain, so that ultrasonic probing is limited to interior points x in Ω' (see the list of notations), where d_0 is very large

compared to the radius of the spot of the ultrasonic perturbation.

We suppose that this deformation affects γ and q *linearly* with respect to the amplitude of the ultrasonic signal. Such an assumption is reasonable if the amplitude is not too large. Thus, when the electric potential is measured while the ultrasonic perturbation is enforced, the equation for the potential is

$$\operatorname{div}(\gamma_w \nabla u_{i,w}) + k_i^2 q_w u_{i,w} = 0 \quad \text{in} \quad \Omega, \tag{4}$$

$$\gamma \frac{\partial u_{i,w}}{\partial \nu} = \varphi_i \quad \text{on} \quad \partial\Omega. \tag{5}$$

with

$$\gamma_w = \gamma + 1_w(\tilde{\gamma}\lambda - \gamma), \tag{6}$$

$$q_w = q + 1_w(\tilde{q}\lambda - q), \tag{7}$$

where λ is the amplitude of the ultrasonic perturbation given by the ratio of the perturbed volume V_w^p of w over the unperturbed one V_w (see [1]). In other words

$$\gamma_w(x) = \begin{cases} \gamma(x), & x \in \Omega \setminus w, \\ \lambda(x)\tilde{\gamma}(x), & x \in w \end{cases} \qquad q_w(x) = \begin{cases} q(x), & x \in \Omega \setminus w, \\ \lambda(x)\tilde{q}(x), & x \in w \end{cases}$$

where $\lambda(x) = V_w^p / V_w$ is a known function.

The analysis of the change of the Neumann-to-Dirichlet map as a result of electromagnetic perturbation of small volume follows [1]. The main differences between the case of the conductivity equation considered in [1] and our case of the Helmholtz equation are the following: this time the boundary data φ and the solutions u_i are complex-valued functions in our case while they are real in [1]) and in our case we need to reconstruct simultaneous two coupled real-valued parameters γ and q. Therefore we expand the main ideas of [1] to our case (see Section 2). The choice of real γ and q implies the existence of eigenfrequencies (see problem (3)) and this gives an additional difficulty in numeric reconstruction. The case of complex γ and q which allows to avoid the resonances, will be considered in [5].

The signature of the perturbations on boundary measurements can be measured by the change of energy on the boundary, namely

$$\int_{\partial\Omega} (u_w - u)\overline{\varphi} d\sigma = |w| \left[\mathbf{M}_w \left(\frac{\tilde{\gamma}\lambda}{\gamma} \right) (\tilde{\gamma}\lambda - \gamma) \nabla u(z) \cdot \overline{\nabla u(z)} - k^2 (\tilde{q}\lambda - q) u(z) \cdot \overline{u(z)} \right]. \tag{8}$$

Assuming the perturbed region is a ball, the polarization tensor $\mathbf{M}_w \left(\frac{\tilde{\gamma}\lambda}{\gamma} \right)$ is a scalar,

$$M_w = (\tilde{\gamma}\lambda - \gamma)/(\tilde{\gamma}\lambda + \gamma).$$

Therefore, for a localized perturbation focused at a point z, we read the following data (rescaled by the volume)

$$D_z(\lambda) = \gamma |\nabla u(z)|^2 \frac{(\frac{\tilde{\gamma}}{\gamma}\lambda - 1)^2}{\frac{\tilde{\gamma}}{\gamma}\lambda + 1} - k^2 q |u(z)|^2 (\frac{\tilde{q}}{q}\lambda - 1). \tag{9}$$

We notice that the data $D_z(\lambda)$ from (9) can be measured for given λ and k thanks

to the identity:

$$D_z(\lambda) = \frac{1}{|w|}\int_{\partial\Omega}(u_w - u)\overline{\varphi}d\sigma.$$

The parameters $\frac{\tilde{\gamma}}{\gamma}(z)$ and $\frac{\tilde{q}}{q}(z)$ are unknown, but the amplitude λ is known. Varying the position of localization, we are able to recover this localized internal data everywhere inside the domain. Thanks to the following lemma [4, 5],

Lemma 1.1: *If the data D_z is known for four distinct values of λ, chosen independently of γ and q, then one can recover $\gamma(z)|\nabla u(z)|^2$ and $q(z)|u(z)|^2$.*

we can find directly the functions $J(z) = \gamma(z)|\nabla u(z)|^2$ and $j(z) = q(z)|u(z)|^2$ for the unique solution u of problem (1)-(2).

The proof of Lemma 1.1 is simply a study of functions of one variable, which is detailed in Appendix A.

The rest of the paper is organized as follows: in Section 2 we prove formula (8), in Section 3 we describe a reconstruction method by perturbations and in Section 4 we give and analyse our numeric results, obtained for two different frequencies and one boundary data in the form of a plane wave.

2. Proof of asymptotic expansion (8)

We suppose that k^2 do not correspond to eigenvalues of problem (3). To prove the asymptotic expansion (8), we first need the following Proposition:

Proposition 2.1: *We have the following identities*

$$\gamma\frac{\partial(u_w - u)}{\partial n} = 0, \tag{10}$$

$$\begin{aligned}&\operatorname{div}(\gamma_w\nabla(u_w - u)) + k^2 q_w(u_w - u)\\ &= -\operatorname{div}(1_w(\gamma_w - \gamma)\nabla u) - k^2 1_w(q_w - q)u,\end{aligned} \tag{11}$$

$$\begin{aligned}&\operatorname{div}(\gamma\nabla(u_w - u)) + k^2 q(u_w - u)\\ &= -\operatorname{div}(1_w(\gamma_w - \gamma)\nabla u_w) - k^2 1_w(q_w - q)u_w,\end{aligned} \tag{12}$$

Thanks to Proposition 2.1, we can estimate the difference between the perturbed and unperturbed solutions $u_w - u$ in $L_2(\Omega)$ by a norm of u in the perturbed region w and by a power of the small volume $|w|$ bigger than 0.5.

Lemma 2.2: *Suppose that $\Omega \subset R^n$ contains a subset of $\Omega' \subset \Omega$ of class C^2, such that $\operatorname{dist}(\Omega', \partial\Omega) > d_0 > 0$, and such that $w \subset \Omega'$. Let q, $\gamma \in L_\infty(\Omega)$ be positive functions, satisfying $0 < c_0 < q(x), \gamma(x) < C_0 < +\infty$ a. e. $x \in \Omega$, and k^2 is not a Neumann eigenvalue for problem (3). Then for the functions u_w and $u \in W^1_\infty$ verifying Eq. (10) and Eq. (11) we have*

$$\|u_w - u\|_{H^1(\Omega)} \leq C|w|^{\frac{1}{2}}|u|_{W^1_\infty(w)}. \tag{13}$$

Therefore, thanks to relation (12), for $m = \max\{2, n\}$ and all κ satisfying $0 < \kappa < \frac{2}{m}$ there exists a positive constant $C > 0$ depending only on Ω', d_0, c_0, and C_0, such that

$$\|u_w - u\|_{L_2(\Omega)} \leq C|w|^{\frac{1}{2}+\kappa}|u|_{W^1_\infty(w)}. \tag{14}$$

Proof. The proof of estimate (13) follows the proofs of Lemma 15.1 and Proposition 15.2 from [2]. Indeed, as soon as $q(x)/\gamma(x)k^2$ is not an eigenvalue for the operator $-\triangle$ in $L_2(\Omega)$ with the homogeneous Neumann boundary condition, in our case problem (1)-(2) has a unique weak solution u in $H^1(\Omega)$ (for every $\phi \in H^{-1/2}(\partial\Omega)$). A_δ is uniformly continuous and uniformly coercive on $H^1 \times H^1$. The embedding $H^1(\Omega) \Subset L_2(\Omega)$ is still compact because $\partial\Omega \in C^2$ and Ω is compact.

For passing to the perturbed problem, we change δ on w (repeat the procedure from [2]) and obtain with the help of relation (11) the desired estimate (13).

Let us prove estimate (14). Select v as the solution to

$$\begin{aligned}
&\operatorname{div}(\gamma\nabla v) + k^2 q v = u_w - u \\
&\gamma\frac{\partial v}{\partial n}|_{\partial\Omega} = 0.
\end{aligned}$$

For this v we have $\|v\|_{H^2(\Omega)} \le C\|u_w - u\|_{L_2(\Omega)}$, and

$$\begin{aligned}
&\int_\Omega |u_w - u|^2 dx = -\int_\Omega \gamma(x)\nabla(u_w - u)\nabla\overline{v}dx + \int_\Omega \omega^2 q(x)(u_w - u)\overline{v}dx \\
&= \int_\Omega \overline{v}\left[\operatorname{div}(\gamma(x)\nabla(u_w - u)) + k^2 q(x)(u_w - u)\right]dx \\
&= -\int_\Omega \overline{v}\left[\operatorname{div}(1_w(\gamma_w - \gamma)\nabla u_w) + k^2 1_w(q_w - q)u_w\right]dx \\
&\le \left|\int_\Omega \overline{v}\left[\operatorname{div}(1_w(\gamma_w - \gamma)\nabla u_w) + k^2 1_w(q_w - q)u_w\right]dx\right| \\
&\le \left|\int_\Omega 1_w(\gamma_w - \gamma)\nabla\overline{v}\nabla u_w dx\right| + \left|\int_\Omega k^2 1_w(q_w - q)\overline{v}u_w dx\right| \\
&\le C\left(\left(\int_w |\nabla u_w|^q dx\right)^{\frac{1}{q}}\left(\int_\Omega |\nabla v|^p dx\right)^{\frac{1}{p}} + \left(\int_w |u_w|^{\tilde{q}} dx\right)^{\frac{1}{\tilde{q}}}\left(\int_\Omega |v|^{\tilde{p}} dx\right)^{\frac{1}{\tilde{p}}}\right) \\
&\le C_p\left(\left(\int_w |\nabla u_w|^q dx\right)^{\frac{1}{q}}\|v\|_{H^2(\Omega)} + \left(\int_w |u_w|^{\tilde{q}} dx\right)^{\frac{1}{\tilde{q}}}\|v\|_{H^1(\Omega)}\right) \\
&\le C_p\left(\left(\int_w |\nabla u_w|^q dx\right)^{\frac{1}{q}} + \left(\int_w |u_w|^{\tilde{q}} dx\right)^{\frac{1}{\tilde{q}}}\right)\|u_w - u\|_{L_2(\Omega)} \qquad (15)
\end{aligned}$$

provided p, $\tilde{p}$ and q, $\tilde{q}$ are related by $\frac{1}{q} + \frac{1}{p} = 1$ and $\frac{1}{\tilde{q}} + \frac{1}{\tilde{p}} = 1$. We use Sobolev's Embedding Theorem to provide the inclusions $H^2 \subset W_p^1$ and $H^1 \subset L_{\tilde{p}}$. We require that q, $\tilde{q} > \frac{2m}{m+2}$, so that $1 < p$, $\tilde{p} < \frac{2m}{m-2}$. For any $1 < \tilde{q} < 2$ (see [3, p.164]) we have

$$\begin{aligned}
&\|u_w\|_{L_{\tilde{q}}(w)} \le \|u_w - u\|_{L_{\tilde{q}}(w)} + \|u\|_{L_{\tilde{q}}(w)} \le \\
&\le \left(\int_w 1dx\right)^{\frac{1}{\tilde{q}} - \frac{1}{2}}\|u_w - u\|_{L_2(w)} + |w|^{\frac{1}{\tilde{q}}}\|u\|_{L_\infty(w)} \\
&\le C|w|^{\frac{1}{\tilde{q}}}\|u\|_{L_\infty(w)}, \qquad (16)
\end{aligned}$$

and for any $1 < q < 2$ we obtain

$$\|\nabla u_w\|_{L_q(w)} \leq C_q |w|^{\frac{1}{q}} \|\nabla u\|_{L_\infty}. \tag{17}$$

A combination of estimations (15), (17) and (16) yields

$$\|u_w - u\|_{L_2(\Omega)} \leq C|w|^{\frac{1}{q}} (|u|_{L_\infty(w)} + |\nabla u|_{L_\infty(w)})$$

for any $\frac{2m}{m+2} < q < 2$. In other words, $\frac{1}{2} < \frac{1}{q} < \frac{m+2}{2m} = \frac{1}{2} + \frac{2}{m}$ with $m = \max\{2, n\}$, from where we can take $\tilde{q} = \frac{1}{q} = \frac{1}{2} + \kappa$ for $0 < \kappa < \frac{2}{m}$. □

In addition of estimates (13) and (14), let us show that the difference $u - u_w$ can be totally described by an integral expression over w.

Proposition 2.3: *Suppose that k^2 is not the Neumann eigenvalue for $\operatorname{div}(\gamma(x)\nabla_x)+q(x)$ on w. Let $N_{\gamma q}(x,z)$ be the Neumann function for $\operatorname{div}(\gamma(x)\nabla_x)+q(x)$ in Ω corresponding to a Dirac mass at z. That is $N_{\gamma q}$ is the solution to*

$$\begin{cases} \operatorname{div}(\gamma(x)\nabla_x N_{\gamma q}(x,z)) + k^2 q(x) N_{\gamma q}(x,z) = -\delta_z, \text{ in } \Omega, \\ \gamma \frac{\partial N_{\gamma q}}{\partial \nu} = 0 \qquad\qquad\qquad\qquad\qquad\qquad \text{on } \partial\Omega. \end{cases} \tag{18}$$

Then, by definition of $N_{\gamma q}$ (which is a real function!), the function U defined by

$$U(x) = \int_{\partial\Omega} N_{\gamma q}(x,z)\varphi(z)d\sigma(z)$$

is the solution of system (1)-(2). Therefore, the solutions u and u_w of systems (1)-(2) and (4)-(25) satisfy

$$(u-u_w)(z) = \int_w (\gamma_w - \gamma)(z)\nabla u_w(z)\nabla_z N_{\gamma q}(z,x)dz + \int_w k^2(q-q_w)(z)u_w(z)N_{\gamma q}(z,x)dz. \tag{19}$$

Proof. Note that the Neumann function $N_{\gamma q}(x,z)$ is defined as a function of $x \in \overline{\Omega}$ for each fixed $z \in \Omega$. Since k^2 is not the Neumann eigenvalue for $\operatorname{div}(\gamma(x)\nabla_x) + q(x)$ on w, the direct problem (1) admits a unique solution u (see [2]). Thus, the solution u is represented by the formula

$$u(x) = \int_{\partial\Omega} N_{\gamma q}(x,z)\varphi(z)d\sigma(z).$$

We notice that

$$\operatorname{div}(\gamma(x)\nabla u_w) + k^2 q(x)u_w = -\operatorname{div}(1_w(\gamma_w - \gamma)(x)\nabla u_w) - k^2 1_w(q_w - q)(x)u_w, \tag{20}$$

We multiply relation (20) by $N_{\gamma q}$ and integrate over Ω:

$$\int_{\partial\Omega} \varphi(z)N_{\gamma q}(x,z)d\sigma(z) - \int_\Omega \gamma(z)\nabla u_w(z)\nabla N_{\gamma q}(x,z)dz + \int_\Omega k^2 q(z)u_w(z)N_{\gamma q}(z,x)dz =$$
$$= \int_\Omega 1_w(z)(\gamma_w - \gamma)(z)\nabla u_w(z)\nabla N_{\gamma q}(x,z)dz - \int_\Omega k^2 1_w(z)(q_w - q)(z)u_w(z)N_{\gamma q}(x,z)dz.$$

Therefore, using $\int_{\partial\Omega} u_w(z)\gamma(z)\nabla N_q(x,z)d\sigma(z) = 0$, from the following equality

$$u(z) + \int_\Omega u_w(z)\left(\mathrm{div}(\gamma(z)\nabla N_{\gamma q}(x,z)) + k^2 q(z) N_{\gamma q}(z,x)\right) dz =$$
$$= \int_\Omega 1_w(z)(\gamma_w - \gamma)(z)\nabla u_w(z)\nabla N_{\gamma q}(x,z)dz + \int_\Omega k^2 1_w(z)(q-q_w)(z)u_w(z)N_{\gamma q}(x,z)dz,$$

we obtain Eq. (19).□

Multiplying Eq. (19) by $\overline{\varphi}(x)$ and integrating over $\partial\Omega$, we find

$$\int_{\partial\Omega}(u-u_w)\overline{\varphi}d\sigma(x) = \int_w (\gamma_w-\gamma)(z)\nabla u_w(z)\nabla_z\left(\int_{\partial\Omega} N_{\gamma q}(z,x)\overline{\varphi}(x)d\sigma(x)\right)dz$$
$$+\int_w k^2(q-q_w)(z)u_w(z)\left(\int_{\partial\Omega} N_{\gamma q}(z,x)\overline{\varphi}(x)d\sigma(x)\right)dz,$$

which gives

$$\int_{\partial\Omega}(u-u_w)\overline{\varphi}d\sigma(x) = \int_w (\gamma_w-\gamma)(z)\nabla u_w(z)\nabla\overline{u}dz + \int_w k^2(q-q_w)(z)\ u_w(z)\overline{u}dz. \tag{21}$$

Remark 1 : [3] Consider a sequence of sets $w_\epsilon \subset\subset \Omega$. Since the family of functions $\frac{1}{|w_\epsilon|}1_{w_\epsilon}$ is bounded in $L_1(\Omega)$, it follows from a combination of the Banach-Alaoglu Theorem and Riesz Representation Theorem that we may find a regular, positive Borel measure μ, and a subsequence w_{ϵ_k}, with $|w_{\epsilon_k}| \to 0$, such that $\frac{1}{|w_\epsilon|}1_{w_\epsilon} \to d\mu$.

Finally, thanks to the a priori estimations (13), (14) and the representation formula (21), we establish the main result:

Lemma 2.4: *Assume that $u \in W^1_\infty(w)$. Consider a sequence of sets $w \subset\subset \Omega$ such that $\frac{1}{|w|}1_w$ converges in the sense of measures to a probability measure $d\mu$ as $|w|$ tends to zero. Then,*

$$\int_{\partial\Omega}(u_w - u)\overline{\varphi}d\sigma = \int_w \mathbf{M}_w(\tilde{\gamma}\lambda-\gamma)|\nabla u|^2dx - k^2|w|\int_w \mathbf{m}_w(\tilde{q}\lambda - q)|u|^2dx + O(|w|^{1+\kappa}). \tag{22}$$

The exponent κ only depends on Ω_1, $\sup_\Omega|q_w|$, $\sup_\Omega|\gamma_w|$, $\inf_\Omega|q_w|$ and $\inf_\Omega|\gamma_w|$. The remainder term has the form

$$|O(|w|^{1+\kappa})| \le C|w|^{1+\kappa}\|u\|_{W^1_\infty(w)}\|\nabla\psi\|_{L_\infty(\Omega)},$$

where C depends only on Ω_1, $\sup_\Omega|q_w|$, $\sup_\Omega|\gamma_w|$, $\inf_\Omega|q_w|$ and $\inf_\Omega|\gamma_w|$. Finally, with a hypothesis that w is a ball, the polarization tensors $\mathbf{M}_w$ and $\mathbf{m}_w$ become the scalar functions M_w and m_w, which are given by

$$M_w = \frac{1}{|w|}1_w(x)\left(\frac{\frac{\tilde{\gamma}}{\gamma}\lambda(x)-1}{\frac{\tilde{\gamma}}{\gamma}\lambda(x)+1}\right) \quad \textit{and} \quad m_w = \frac{1}{|w|}1_w(x).$$

Proof. Suppose that k^2 is not a Neumann eigenvalue for problem (3). We have relation (21). We are looking for an approximation of the terms of Eq. (21) depending on u_w by a function depending on u. In the same way as in [1], we introduce

the solution ζ_w of the following problem

$$\begin{cases} \operatorname{div}(\gamma_w(x)\nabla\zeta_w) + k^2 q_w(x)\zeta_w = \operatorname{div}(\gamma(x)\nabla_x\zeta) + k^2 q(x)\zeta & \text{in } \Omega, \\ \gamma\frac{\partial\zeta_w}{\partial n} = \gamma\frac{\partial\zeta}{\partial n} & \text{on } \partial\Omega. \end{cases}$$

Corresponding to ζ_w, we define in the unperturbed case $\zeta = x + C + i(x + \tilde{C})$, where C and $\tilde{C}$ are constants in $\mathbb{R}^d$ for $x \in \mathbb{R}^d$. This time all functions ζ, ζ_w, u and u_w are complex. The choice of C ($\tilde{C}$) will be discussed later. Thanks to Lemma 2.2, for $\zeta_w - \zeta$ we still have an analogue version of Proposition 3.1 of [1, p.6]:

Proposition 2.5: *Consider a sequence of sets $w \subset\subset \Omega$, such that $\frac{1}{|w|}1_w$ converges in the sense of measures to a probability measure $d\mu$ as $|w|$ tends to zero. Then, the corrector $\frac{1}{|w|}1_w\frac{\partial\zeta_w}{\partial x_j}$ converges in the sense of measures to $M_j d\mu$ (M_j is a scalar function). Furthermore, it satisfies*

$$\|\nabla(\zeta_w - \zeta)\|_{L_2(\Omega)} \leq C|w|^{\frac{1}{2}} \quad \textit{and } \|\zeta_w - \zeta\|_{L_2(\Omega)} \leq C|w|^{\frac{1}{2}+\kappa},$$

where the constants $\kappa > 0$ and $C > 0$ depend only on Ω_1, $\sup_\Omega |q_w|$, $\sup_\Omega |\gamma_w|$, $\inf_\Omega |q_w|$ and $\inf_\Omega |\gamma_w|$.

The rest of the proof follows the analogous one given in details in [1]. This time the remaining term is bounded by

$$|O(|w|^{1+\kappa})| \leq C|w|^{1+\kappa}\|u\|_{W^1_\infty(w)}\|\psi\|_{W^1_\infty(\Omega)}.$$

We also remark (see [1] for the notations) that the choice of $\psi_i = \frac{\partial}{\partial x_i}u \star \eta$ (where η is the standard mollifier) determine the constants $C = (C_1, \ldots, C_d)$ and $\tilde{C} = (\tilde{C}_1, \ldots, \tilde{C}_d)$ in the definition of the function $\zeta(z)$:

$$C_j + i\tilde{C}_j = \frac{\overline{u}(z_0) - z_0\frac{\partial}{\partial x_i}\overline{u}(z_0)}{\frac{\partial}{\partial x_i}\overline{u}(z_0)} \quad \text{for a } z_0 \in w,$$

which ensures that $\zeta(z)\overline{\psi} \approx \overline{u}(z)$.

Finally, we deduce

$$\begin{aligned} &\int_{\partial\Omega}(u - u_w)\overline{\varphi}d\sigma(x) \\ &= |w|\int_w \mathbf{M}_w(\gamma_w - \gamma)(z)|\nabla u(z)|^2 dz + |w|\int_w k^2\frac{1_w}{|w|}(q - q_w)(z)|u(z)|^2 dz + O(|w|^{1+\kappa}), \end{aligned}$$

with $M_w = \frac{1}{|w|}1_w(x)\left(\frac{\frac{\tilde{\gamma}}{\gamma}\lambda(x)-1}{\frac{\tilde{\gamma}}{\gamma}\lambda(x)+1}\right)$ if w is a sphere. This proves relation (8) and provide the existence of a known function $D_z(\lambda)$ from (9). □

3. Reconstruction γ and q by a perturbative method. Numeric algorithm

We consider the system of Helmholtz equations with different frequencies $k_1 \neq k_2$:

$$\operatorname{div}(\gamma(x)\nabla u_{k_1}) + k_1^2 q(x) u_{k_1} = 0 \qquad \text{in } \Omega, \tag{23}$$

$$\operatorname{div}(\gamma(x)\nabla u_{k_2}) + k_2^2 q(x) u_{k_2} = 0 \qquad \text{in } \Omega, \tag{24}$$

$$u_{k_1} = u_{k_2} = \psi \qquad \text{on } \partial\Omega. \tag{25}$$

The data ψ is the Dirichlet data measured as a response to the current φ in absence of elastic deformation. We take $\psi = e^{i \arctan y/x}$, which represents a plane wave.

We use the following formulas $\gamma(x)|\nabla u_{k_1}|^2 = J_{k_1}(x)$ and $q(x)|u_{k_2}|^2 = j_{k_2}(x)$. Thus, we can approximate our problem by system (26) and (27)

$$\operatorname{div}\left(\frac{J_{k_1}(x)}{|\nabla u_{k_1}|^2}\nabla u_{k_1}\right) + k_1^2 q(x) u_{k_1} = 0 \qquad \text{in } \Omega, \tag{26}$$

$$\operatorname{div}(\gamma(x)\nabla u_{k_2}) + k_2^2 \frac{j_{k_2}(x)}{|u_{k_2}|^2} u_{k_2} = 0 \qquad \text{in } \Omega, \tag{27}$$

where it is supposed that

$$|\nabla u_{k_1}|^2 > 0 \quad \text{and} \quad |u_{k_2}|^2 > 0 \quad \text{for all} \quad x \in \Omega.$$

Let us explain the steps of the numeric algorithm. The method uses two sub-algorithms to reconstruct γ for a fixed q (constant for the ultrasound perturbation) and to reconstruct q for a fixed γ (constant).

First we notice that we have two frequencies k_1 and k_2.

Step 0. We construct the functions J_{k_1} and j_{k_2}.

Step 1. We take an initial guess q_0 and γ_0.

Step 2. In the aim of updating first γ_0 we solve the linear system for chosen q_0 and γ_0 and the frequency k_1:

$$\begin{cases} \operatorname{div}(\gamma_0 \nabla u_{k_1}) + k_1^2 q_0 u_{k_1} = 0 \\ u_{k_1}|_{\partial\Omega} = \psi \end{cases}$$

We obtain the solution of this system which we denote by u_{0k_1}. Knowing the approximate solution u_{0k_1}, we calculate the error on γ:

$$E_{0k_1} = \frac{J_{k_1}}{|\nabla u_{0k_1}|^2} - \gamma_0.$$

Step 3. We verify the condition $|E_{0k_1}| < \epsilon_{\text{precision}}$ for a given positive constant $\epsilon_{\text{precision}}$, which gives the desired order of the precision of the final result. If $|E_{0k_1}|$ is smaller than $\epsilon_{\text{precision}}$, we take $\gamma \equiv \gamma_0$ and go to Step 5 for the reconstruction of q, otherwise we go to Step 4.

Step 4. We apply the algorithm described in details in Subsection 3.1 to determine the correctors $\delta\gamma_1$ and δu_{1k_1} for a fixed q_0 and to update γ_0 using formula (35).

Step 5. In the aim of updating q_0, we solve the following linear system with the frequency k_2 for a chosen q_0 and γ_0 updated on Step 4:

$$\begin{cases} \operatorname{div}(\gamma_0 \nabla u_{k_2}) + k_2^2 q_0 u_{k_2} = 0 \\ u_{k_2}|_{\partial\Omega} = \psi \end{cases}$$

We obtain the solution of this system which we denote by u_{0k_2}. Knowing the approximate solution u_{0k_2}, we calculate the error on q:

$$e_{0k_2} = \frac{j_{k_2}}{|u_{0k_2}|^2} - q_0.$$

Step 6. We verify the condition $|e_{0k_2}| < \epsilon_{\text{precision}}$. If $|e_{0k_2}|$ is smaller than $\epsilon_{\text{precision}}$, we take $q \equiv q_0$ and finish the algorithm, otherwise we do Step 7.

Step 7. We apply the algorithm described in details in Subsection 3.2 to determinate the correctors δq_1 and δu_{1k_2} for a fixed γ_0 and to update q_0 using formula (40). Next we go to Step 2.

3.1. *Algorithm of reconstruction of γ for a constant q*

Step 1. We start from an initial guess γ_0, and solve the corresponding Dirichlet problem for the Helmholtz equation

$$\begin{aligned} &\operatorname{div}(\gamma_0(x)\nabla u_0) + k^2 q u_0 = 0, \\ &u_0|_{\partial\Omega} = \psi. \end{aligned}$$

Solving the direct problem for $\psi = e^{i \arctan y/x}$, we obtain u_0.

Step 2. We have seen that our inverse problem is asymptotically approached by the direct problem

$$\begin{cases} \operatorname{div}(\frac{J(x)}{|\nabla u|^2}\nabla u) + \omega^2 q u = 0, \text{ in } \Omega, \\ u = \psi, \qquad\qquad\qquad\quad \text{on } \partial\Omega. \end{cases} \tag{28}$$

We compute the difference

$$E_0 := \frac{J(x)}{|\nabla u_0|^2} - \gamma_0 \tag{29}$$

and verify

$$|E_0| < C_{\text{prec}}, \tag{30}$$

where C_{prec} is our wished order of the precision. If condition (30) holds, we finish our algorithm and set $\gamma \equiv \gamma_0$. Otherwise we go to the next step.

Step 3. We use now the expression

$$(\gamma_0 + \delta\gamma_1)|\nabla(u_0 + \delta u_1)|^2 = J(x),$$

having the goal to approximate the known function $J(x)$ with the help of the small correctors δu_1 and $\delta\gamma_1$. We suppose that $\delta \ll 1$ and that $\delta \max_x |\gamma_1|$ and $\delta \max_x |u_1|$ are of the order of δ.

By expanding the expression, we obtain

$$\begin{aligned} &\delta\gamma_1 \left(1 + 2\delta \left(\frac{\nabla(\operatorname{Re} u_0)\nabla(\operatorname{Re} u_1) + \nabla(\operatorname{Im} u_0)\nabla(\operatorname{Im} u_1)}{|\nabla u_0|^2}\right) + \delta^2 \frac{|\nabla u_1|^2}{|\nabla u_0|^2}\right) = \frac{J(x)}{|\nabla u_0|^2} - \gamma_0 \\ &-2\delta \frac{\gamma_0 \left(\nabla(\operatorname{Re} u_0)\nabla(\operatorname{Re} u_1) + \nabla(\operatorname{Im} u_0)\nabla(\operatorname{Im} u_1)\right)}{|\nabla u_0|^2} - \delta^2 \gamma_0 \frac{|\nabla u_1|^2}{|\nabla u_0|^2}. \end{aligned}$$

We consider only terms of order not smaller than δ:

$$\delta\gamma_1 = \frac{J(x)}{|\nabla u_0|^2} - \gamma_0 - 2\delta\frac{\gamma_0\left(\nabla(\operatorname{Re} u_0)\nabla(\operatorname{Re} u_1) + \nabla(\operatorname{Im} u_0)\nabla(\operatorname{Im} u_1)\right)}{|\nabla u_0|^2}.$$

To find the corrector $\tilde{u}_1 = \delta u_1$, we expand the following equation

$$\operatorname{div}((\gamma_0 + \delta\gamma_1)\nabla(u_0 + \delta u_1)) + k^2 q(u_0 + \delta u_1) = 0.$$

By considering the terms of order not smaller than δ and by replacing $\delta\gamma_1$ by the approximated formula, we can find $\tilde{u}_1$ as the solution of the following problem

$$\operatorname{div}\left[\gamma_0\left(\nabla\tilde{u}_1 - 2\frac{\nabla u_0}{|\nabla u_0|^2}\left(\nabla \operatorname{Re} u_0 \nabla \operatorname{Re}\tilde{u}_1 + \nabla \operatorname{Im} u_0 \nabla \operatorname{Im}\tilde{u}_1\right)\right)\right] \tag{31}$$

$$+ \operatorname{div}(E_0\nabla\tilde{u}_1) + \operatorname{div}(E_0\nabla u_0) + k^2 q\tilde{u}_1 = 0,$$

$$\tilde{u}_1|_{\partial\Omega} = 0. \tag{32}$$

Let us define

$$\boldsymbol{GU}_0 = \begin{pmatrix}\nabla \operatorname{Re} u_0 \\ \nabla \operatorname{Im} u_0\end{pmatrix} \quad \text{and} \quad \boldsymbol{GU}_1 = \begin{pmatrix}\nabla \operatorname{Re}\tilde{u}_1 \\ \nabla \operatorname{Im}\tilde{u}_1\end{pmatrix},$$

and suppose that

$$\boldsymbol{U}_0 = \begin{pmatrix}\operatorname{Re} u_0 \\ \operatorname{Im} u_0\end{pmatrix} \quad \text{and} \quad \boldsymbol{U}_1 = \begin{pmatrix}\operatorname{Re}\tilde{u}_1 \\ \operatorname{Im}\tilde{u}_1\end{pmatrix},$$

thus we have

$$\nabla \operatorname{Re} u_0 \nabla \operatorname{Re}\tilde{u}_1 + \nabla \operatorname{Im} u_0 \nabla \operatorname{Im}\tilde{u}_1 = \boldsymbol{GU}_0 \cdot \boldsymbol{GU}_1^T.$$

We also use the relation

$$|\nabla u_0|^2 = |\boldsymbol{GU}_0|^2.$$

We solve problem (31)-(32) for the real and imaginary parts of $_1$ and using our notations we obtain the system

$$\operatorname{div}\left[\gamma_0\left(\boldsymbol{GU}_1 - 2\frac{\boldsymbol{GU}_0}{|\boldsymbol{GU}_0|}\left(\frac{\boldsymbol{GU}_0}{|\boldsymbol{GU}_0|}\cdot\boldsymbol{GU}_1\right)\right)\right]$$

$$+ \operatorname{div}(E_0\boldsymbol{GU}_1) + \operatorname{div}(E_0\boldsymbol{GU}_0) + k^2 q\boldsymbol{U}_1 = 0,$$

$$\boldsymbol{U}_1|_{\partial\Omega} = 0.$$

The vector $\boldsymbol{\theta}_0 = \frac{\boldsymbol{GU}_0}{|\boldsymbol{GU}_0|}$ is a unit vector. We can rewrite our system in the form

$$\operatorname{div}\left[\gamma_0\left(\mathbf{Id} - \mathbf{2}\boldsymbol{\theta_0}\otimes\boldsymbol{\theta_0}\right)\boldsymbol{GU}_1\right] + \operatorname{div}(E_0\boldsymbol{GU_1}) + \operatorname{div}(E_0\boldsymbol{GU}_0) + k^2 q\boldsymbol{U}_1 = 0,$$

or using eigenvectors

$$\operatorname{div}\left[\gamma_0\left(\boldsymbol{\theta}_0^{\perp}\otimes\boldsymbol{\theta}_0^{\perp} - \boldsymbol{\theta}_0\otimes\boldsymbol{\theta}_0\right)\boldsymbol{GU}_1\right] + \operatorname{div}(E_0\boldsymbol{GU}_1) + \operatorname{div}(E_0\boldsymbol{GU}_0) + k^2 q\boldsymbol{U}_1 = 0.$$

We suppose that $\boldsymbol{GU}_1 \parallel \boldsymbol{\theta}_0$ and obtain

$$-\operatorname{div}(\gamma_0 \nabla \operatorname{Re}\tilde{u}_1) + \operatorname{div}(E_0 \nabla \operatorname{Re}\tilde{u}_1) + \operatorname{div}(E_0 \nabla \operatorname{Re} u_0) + k^2 q \operatorname{Re}\tilde{u}_1 = 0, \quad (33)$$

$$\operatorname{Re}\tilde{u}_1|_{\partial\Omega} = 0;$$

$$-\operatorname{div}(\gamma_0 \nabla \operatorname{Im}\tilde{u}_1) + \operatorname{div}(E_0 \nabla \operatorname{Im}\tilde{u}_1) + \operatorname{div}(E_0 \nabla \operatorname{Im} u_0) + k^2 q \operatorname{Im}\tilde{u}_1 = 0, \quad (34)$$

$$\operatorname{Im}\tilde{u}_1|_{\partial\Omega} = 0.$$

This gives $\tilde{u}_1$.

Step 4. We calculate

$$\tilde{\gamma} = \gamma_0 + \delta\gamma_1 = \frac{1}{|\nabla u_0|^2}\left(J(x) - 2\gamma_0(\nabla \operatorname{Re} u_0 \nabla \operatorname{Re} \nabla\tilde{u}_1 + \nabla \operatorname{Im} u_0 \nabla \operatorname{Im} \nabla\tilde{u}_1)\right). \quad (35)$$

We set now $\gamma_0 \equiv \tilde{\gamma}$, and return to the first step to find the corresponding u_0 and repeat the procedure.

3.2. *Algorithm of reconstruction of q for a constant γ*

Step 1. We start from an initial guess q_0, and solve the corresponding Dirichlet problem for the Helmholtz equation

$$\gamma\triangle u_0 + k^2 q_0(x) u_0 = 0,$$
$$u_0|_{\partial\Omega} = \psi.$$

Solving the direct problem for $\psi = e^{i \arctan y/x}$, we obtain u_0.

Step 2. We have seen that our inverse problem is asymptotically approached by the direct problem

$$\begin{cases} \gamma\triangle u + \omega^2 \frac{j(x)}{|u|^2} u = 0, \text{ in } \Omega, \\ u = \psi, \qquad\qquad\qquad \text{on } \partial\Omega. \end{cases} \quad (36)$$

We compute the difference

$$\epsilon_0 := \frac{j(x)}{|u_0|^2} - q_0 \quad (37)$$

and verify

$$|\epsilon_0| < C_{\text{prec}}, \quad (38)$$

where C_{prec} is our wished order of precision. If condition (38) holds, we finish our algorithm and set $q \equiv q_0$. Otherwise we go to the next step.

Step 3. We use now the expression

$$(q_0 + \delta q_1)|u_0 + \delta u_1|^2 = j(x),$$

having the goal to approximate the known function $j(x)$ with the help of the small correctors δu_1 and δq_1.

By expanding the expression, we obtain

$$\delta q_1 \left(1 + 2\delta \left(\frac{\operatorname{Re} u_0 \operatorname{Re} u_1 + \operatorname{Im} u_0 \operatorname{Im} u_1}{|u_0|^2}\right) + \delta^2 \frac{|u_1|^2}{|u_0|^2}\right) = \frac{j(x)}{|u_0|^2} - q_0$$
$$-2\delta \frac{q_0 \left(\operatorname{Re} u_0 \operatorname{Re} u_1 + \operatorname{Im} u_0 \operatorname{Im} u_1\right)}{|u_0|^2} - \delta^2 q_0 \frac{|u_1|^2}{|u_0|^2}.$$

As in Section 3.1, we suppose that $\delta \ll 1$ and that $\delta \max_x |q_1|$ and $\delta \max_x |u_1|$ are of the order of δ. Consequently, we consider only terms of order not smaller than δ:

$$\delta q_1 = \frac{j(x)}{|u_0|^2} - q_0 - 2\delta \frac{q_0 \left(\operatorname{Re} u_0 \operatorname{Re} u_1 + \operatorname{Im} u_0 \operatorname{Im} u_1\right)}{|u_0|^2}.$$

To find the corrector $\tilde{u}_1 = \delta u_1$, we expand the following equation

$$\gamma \triangle (u_0 + \delta u_1) + k^2 (q_0 + \delta q_1)(u_0 + \delta u_1) = 0.$$

Considering the terms of order no smaller than δ and replacing δq_1 by the approximated formula, we find $\tilde{u}_1$ as a solution of the following problem

$$\gamma \triangle \tilde{u}_1 + k^2 \frac{j(x)}{|u_0|^2} \tilde{u}_1 - 2k^2 u_0 \frac{q_0 \left(\operatorname{Re} u_0 \operatorname{Re} \tilde{u}_1 + \operatorname{Im} u_0 \operatorname{Im} \tilde{u}_1\right)}{|u_0|^2} = -\epsilon_0 k^2 u_0, \quad (39)$$
$$\tilde{u}_1|_{\partial\Omega} = 0.$$

We solve the problem and obtain $\tilde{u}_1$.

Step 4. We calculate

$$\tilde{q} = q_0 + \delta q_1 = \frac{1}{|u_0|^2} \left(j(x) - 2q_0 (\operatorname{Re} u_0 \operatorname{Re} \tilde{u}_1 + \operatorname{Im} u_0 \operatorname{Im} \tilde{u}_1)\right). \quad (40)$$

We set now $q_0 \equiv \tilde{q}$, and return to the first step to find the corresponding u_0 and repeat the procedure.

4. Numerical results

To study the efficiency of this approach, we have tested this method on various problems and domains, using the partial differential equation solver FreeFem++ [6]. We present here one such test. The domain Ω is a disk of radius 8 centred at the origin, which contains three inclusions: a triangle, an L-shaped domain and an ellipse, which represents a convex object, a non-convex object, and an object with a smooth boundary respectively. In Figure 1 (a) (respectively (b)) the background conductivity (respectively permittivity) is equal to 1 (respectively 3), the conductivity (respectively permittivity) takes the value 2.5 (respectively 2) in the triangle, 1.75 (respectively 1) in the ellipse and 3.05 (respectively 2.55) in the L-shaped domain for the two frequencies $k_1 = \pi \cdot 10^3$ and $k_2 = \pi \cdot 10^{-3}$. We purposely choose values corresponding to small and large contrast with the background. The initial guess in Figure 1 (c) (respectively (d)) is equal to 3.5 (respectively 11.5) inside the disk of radius 6 centred at the origin, and equal to the supposedly known conductivity (permittivity) 1 (respectively 3) near the boundary (outside the disk of radius 6). Figure 2 shows the result of the reconstruction when perfect measures (with "infinite" precision) are available. For all presented numerical results

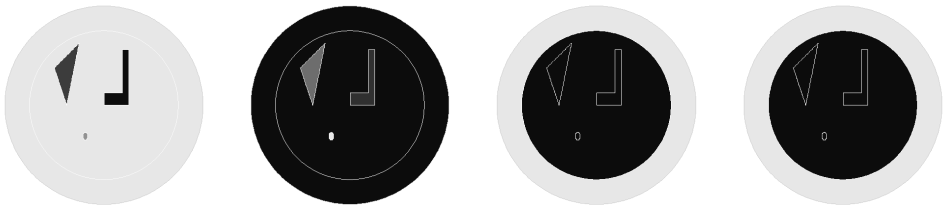

(a) (b) (c) (d)

Figure 1. (a) Distribution of the conductivity γ. (b) Distribution of the permittivity q. (c) Initial guess for γ. (d) Initial guess for q.

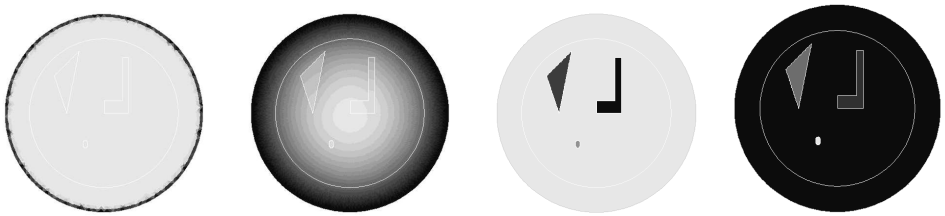

(a) (b) (c) (d)

Figure 2. Reconstruction test with a "perfect" mesh. (a) Collected data J for the reconstruction of γ. (b) Collected data j for the reconstruction of q. (c) Reconstructed conductivity γ. (d) Reconstructed permittivity q.

we use as boundary potential $\psi = e^{i \arctan(x/y)}$. Figure 2 (a) and (b) represents the collected data, $J(x)$ and $j(x)$. For known values of the contrast, we remark that through we can 'see' the structure of the permittivity. On Figures 2 (c) and (d), the reconstructed conductivity and permittivity are represented: they perfectly match the target. Figure 4 (a) (respectively 4 (b)) presents different errors as functions of the iteration for γ (respectively q).

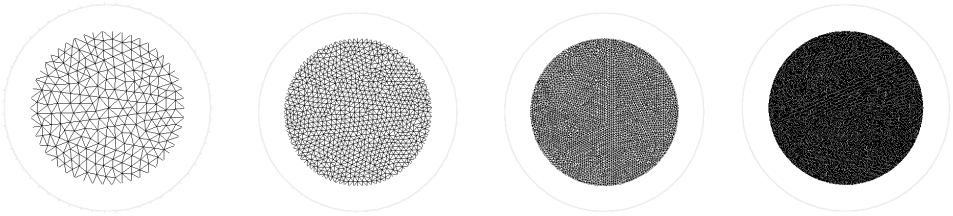

(a) (b) (c) (d)

Figure 3. "Imperfect" meshes for: (a) 50 boundary points; (b) 100 boundary points; (c) 200 boundary points; and (d) 400 boundary points.

We have also considered imperfect data. We ran the reconstruction algorithm with the same conditions, but now assume that the data was measured at the nodes of a regular mesh on the disk, with 50, 100, 200 and 400 boundary points (see meshes on Figure 3). Figure 5 shows the obtained reconstructions, which still perfectly match the target. The convergence result for different number of boundary points is given on Figure 6 for the errors $\|j/|u|^2 - q\|_{L_\infty}$ and $\|J/|\nabla u|^2 - \gamma\|_{L_\infty}$. We can observe that the convergence is exponential and that it is even more faster for meshes of 50 and 100 boundary points than for meshes of 200 or 400 boundary points.

This better convergence for meshes with 50 and 100 boundary points can be

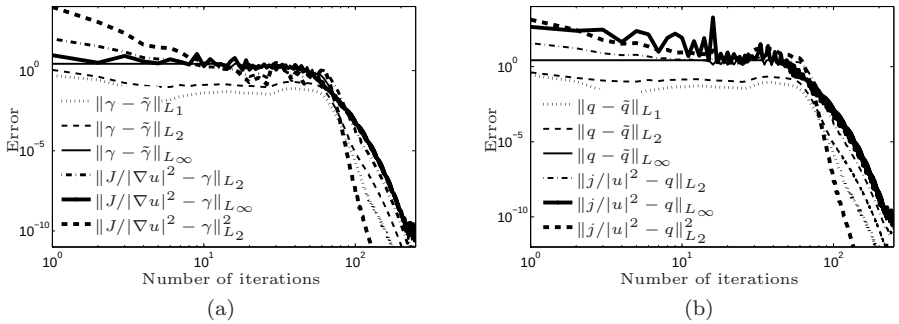

Figure 4. Convergence results for a "perfect" mesh on (a) γ and (b) q.

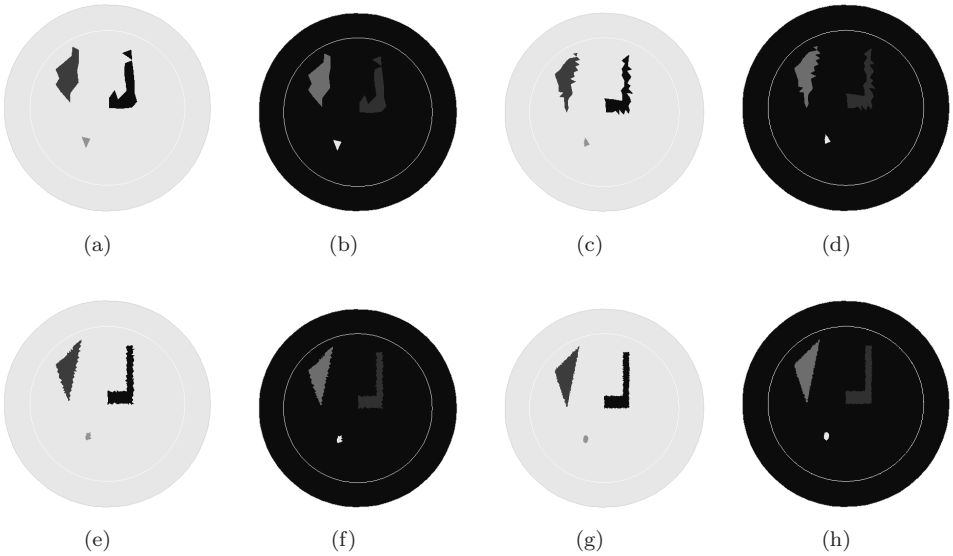

Figure 5. Reconstruction tests for different "imperfect" meshes: (a) γ and (b) q using a regular mesh with 50 boundary points, (c) γ and (d) q using a regular mesh with 100 boundary points, (e) γ and (f) q using a regular mesh with 200 boundary points and (g) γ and (h) q using a regular mesh with 400 boundary points.

illustrated by the following example. For all types of mesh we can perfectly reconstruct γ and q by the perturbative method if one of the chosen frequency (for the reconstruction of γ) is big enough and the second frequency (for the reconstruction of q) is small enough. In the previous examples, the frequencies were chosen equal to $k_1 = \pi \times 10^3$ and $k_2 = \pi \times 10^{-3}$. During our numeric simulations, we have noticed that the smaller $|k_1 - k_2|$ becomes, less efficient the convergence. More precisely, the algorithm does not converge for $|k_1 - k_2| \leq 10$ for the case of meshes with 200 and 400 boundary points (see Figure (7)).

Let us analyse the explanation of these results. We notice that there are two necessary conditions to be satisfied to ensure the convergence of the algorithm by perturbations:

(1) Using the approximation $\gamma(x) = \frac{J(x)}{|\nabla u(x)|^2}$ and $q(x) = \frac{j(x)}{|u(x)|^2}$, we need to ensure that there exist $\delta_1 > 0$ and $\delta_2 > 0$ such that for each iteration step for $l = 1, 2, \ldots$, $|\nabla u^l_{k_i}(x)|^2 > \delta_1$ and $|u^l_{k_i}(x)|^2 > \delta_2$ (where k_i are the chosen frequencies). In other words, we need that the sequences $\{|\nabla u^l_{k_i}(x)|^2 : l = 1, 2 \ldots\}$ and $\{|u^l_{k_i}(x)|^2 : l = 1, 2 \ldots\}$ have some uniform positive lower

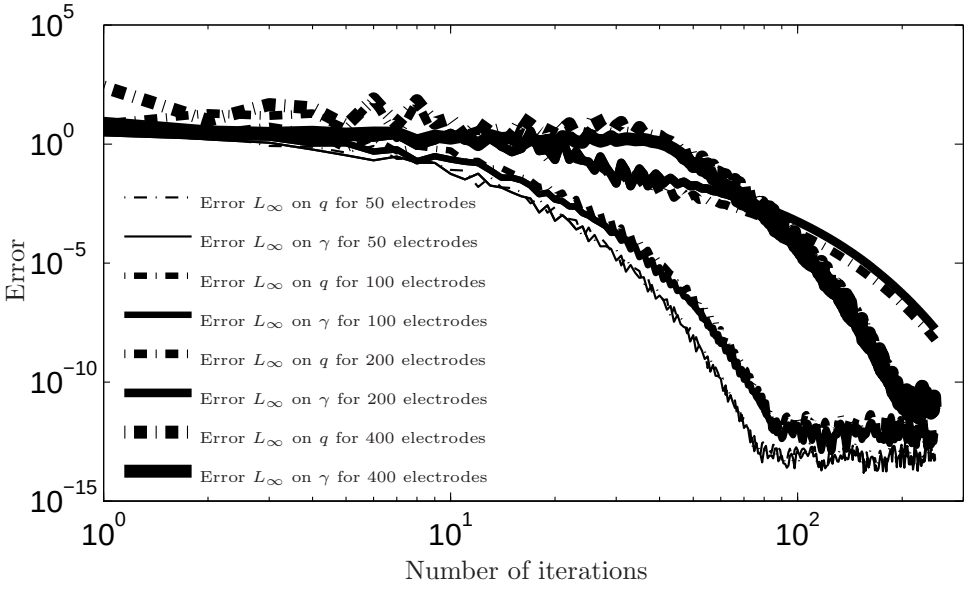

Figure 6. Convergence results. Errors $\|j/|u|^2 - q\|_{L_\infty}$ and $\|J/|\nabla u|^2 - \gamma\|_{L_\infty}$ for meshes with different number of boundary points on q and γ.

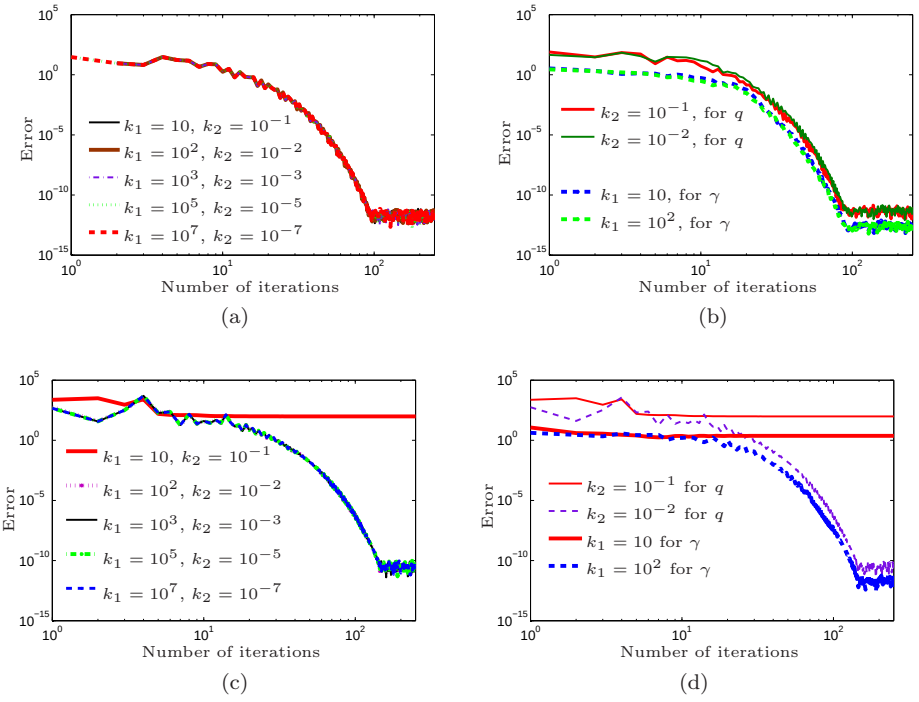

Figure 7. Dependence of the errors $\|J_{k_1}/|\nabla u|^2 - \gamma\|_{L_\infty}$ and $\|j_{k_2}/|\nabla u|^2 - q\|_{L_\infty}$ on the values of k_1, k_2. (a) Case of 50 points on the boundary. (b) Case of 100 points on the boundary. (c) Case of 200 points on the boundary. (d) Case of 400 points on the boundary.

bound.

(2) The corrector functions to update the initial guess for γ and q should be small enough ($|\tilde{u}_1^l| = \delta|u_1| \ll 1$) and for $l \to \infty$, $|\tilde{u}_1^l|$ should tends to 0.

Indeed, if the first condition does not hold, we have a division by zero and the

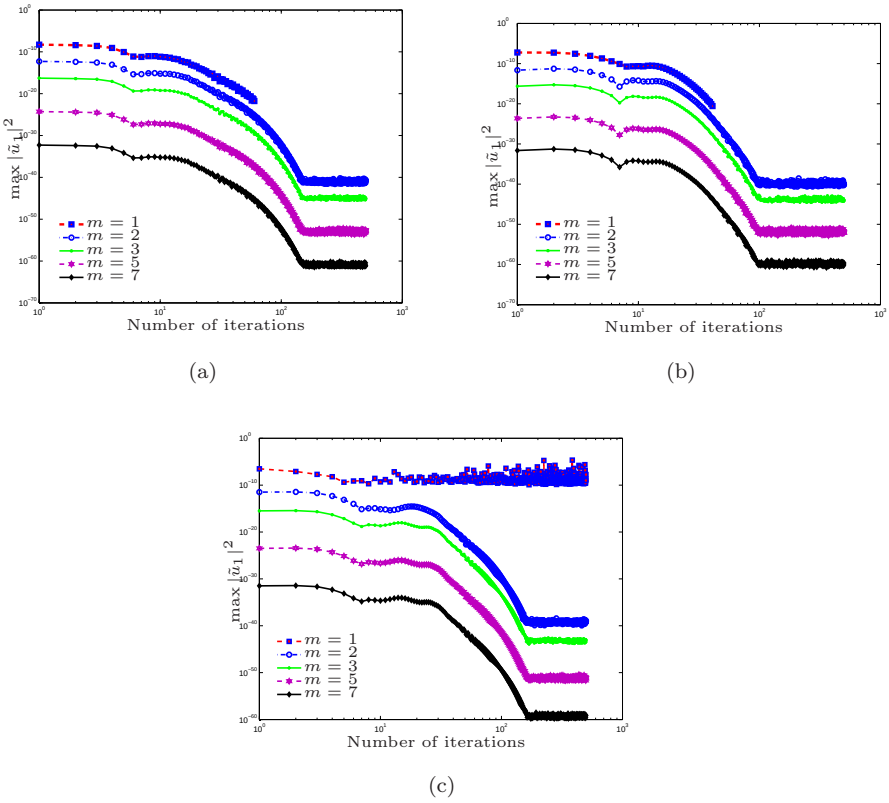

Figure 8. Plot of $\max|\tilde{u}_1|^2$ versus the number of iterations for different values of $k_1 = \pi \times 10^m$, where $\tilde{u}_1$ is the corrector in the reconstruction of γ. (a) Case of 50 points on the boundary. (b) Case of 100 points on the boundary. (c) Case of 200 points on the boundary.

algorithm has no any sense. In the second condition, the smallness of the correctors functions $\tilde{u}_1^l$ is the basic assumption for deriving the approximate systems (33)-(34) and (39) which avoid all the terms of the second order on δ. If $|\tilde{u}_1^l|$ is not small enough, we cannot do it any more and the solutions of systems (33)-(34) and (39) have no any sense. Moreover, the algorithm converges if and only if $|\tilde{u}_1^l| \to 0$ for $l \to \infty$.

Figure 8 shows the decay behaviour of the upper bound of $|\tilde{u}_1^l|^2$ for the corrector $\tilde{u}_1^l$ from the conductivity update algorithm (see system (33)-(34)) for different frequencies and meshes. We observe that we have a good convergence corresponding to the logarithmic decay of $|\tilde{u}_1^l|^2$ for all frequencies and meshes with 50 and 100 boundary points, but we have a divergence result corresponding to the non-decay of $|\tilde{u}_1^l|^2$ for the frequency $k_1 = 10\pi$ and for the mesh with 200 boundary points. The corrector function $\tilde{u}_1^l$ for the reconstruction of q in our numerical tests for $k_2 = \pi \times 10^{-m}$, $m = 1, 2, 3, 5, 7$, is equal to zero. This means that at each iteration step we update q_0 by $\frac{j(x)}{|u_{k_i}^l(x)|^2}$.

To understand why for $k_1 = 10\pi$ and $k_2 = 0.1\pi$ the algorithm diverges for a mesh of 200 boundary points and converges for a mesh of 50 or 100 boundary points, let us verify the first condition of the convergence. Figure 9 (respectively Figure 10) shows the lower bounds of $|\nabla u_{k_i}^l(x)|^2$ and $|u_{k_i}^l(x)|^2$ for different k_1 (respectively k_2) and for different meshes. We notice that we have for all cases, except the case for $k_1 = 10\pi$, $k_2 = 0.1\pi$ and for the mesh with 200 boundary points, that the sequences $\{\min_x |\nabla u_{k_i}^l(x)|^2 : l = 1, 2 \ldots\}$ and $\{\min_x |u_{k_i}^l(x)|^2 : l = 1, 2 \ldots\}$ converge for $l \to \infty$ to a positive constant. Therefore, we see that for $k_1 = 10\pi$ and $k_2 = 0.1\pi$ we

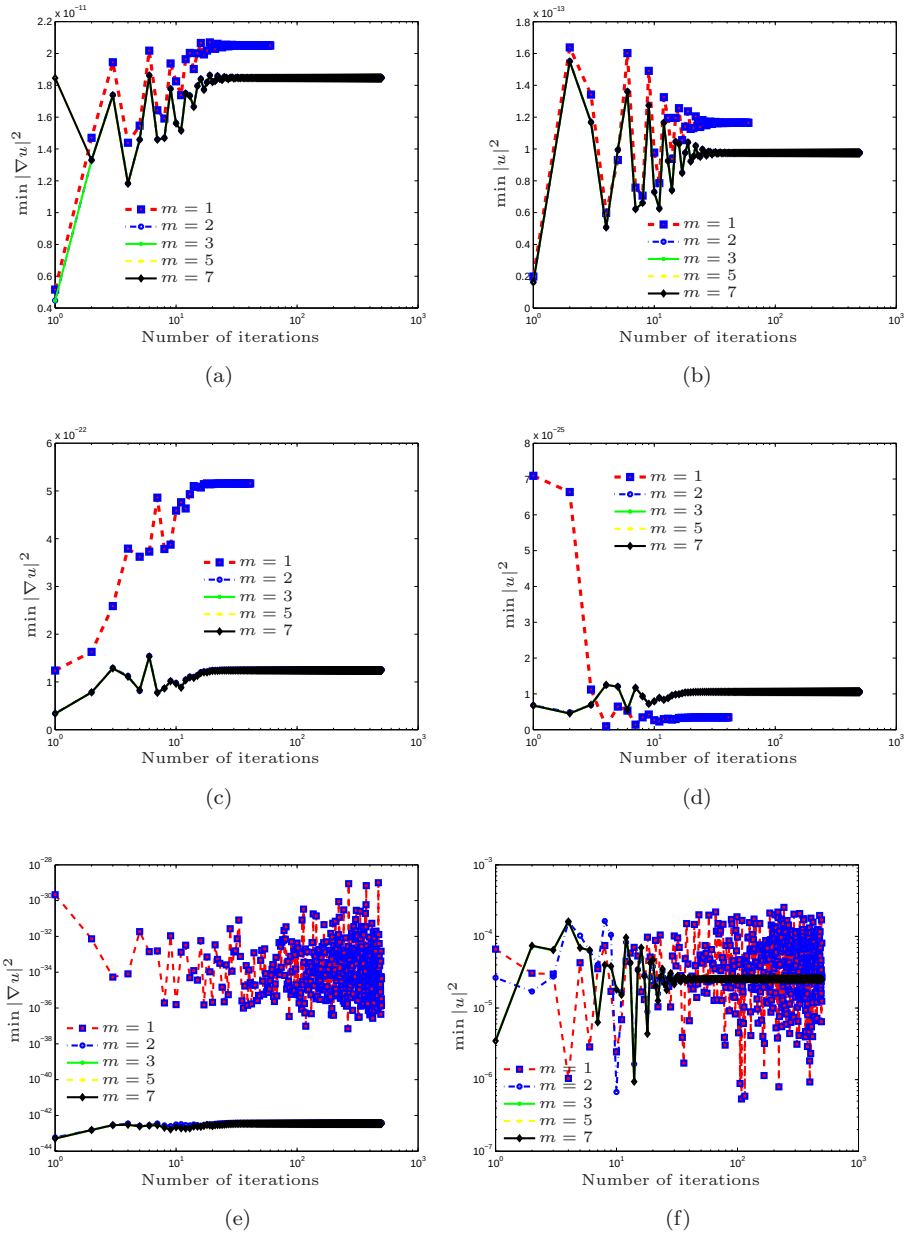

Figure 9. Plot of $\min|\nabla u|^2$ and $\min|u|^2$ versus the number of iterations for different values of $k_1 = \pi \times 10^m$, where u is the numeric solution of the Helmholtz problem. (a) and (b) Case of 50 points on the boundary. (c) and (d) Case of 100 points on the boundary. (e) and (f) Case of 200 points on the boundary.

obtain a divergence of the quantities $\frac{J(x)}{|\nabla u^l_{k_i}(x)|^2}$ and $\frac{j(x)}{|u^l_{k_i}(x)|^2}$. The divergence does not take place for a small number of boundary points because of a lower order of the precision. For example, we notice that with the growth of the number of boundary points (*i.e.* with the growth of the precision) the limits of the sequences $\{\min_x |\nabla u^l_{k_i}(x)|^2 : l = 1, 2\ldots\}$ and $\{\min_x |u^l_{k_i}(x)|^2 : l = 1, 2\ldots\}$ becomes more and more smaller, as illustrated on Figure 11 for $\min_x |u^l_{k_1}|^2$. In the case the mesh of 400 boundary points, the divergence stops the numeric test by the error of the division by zero.

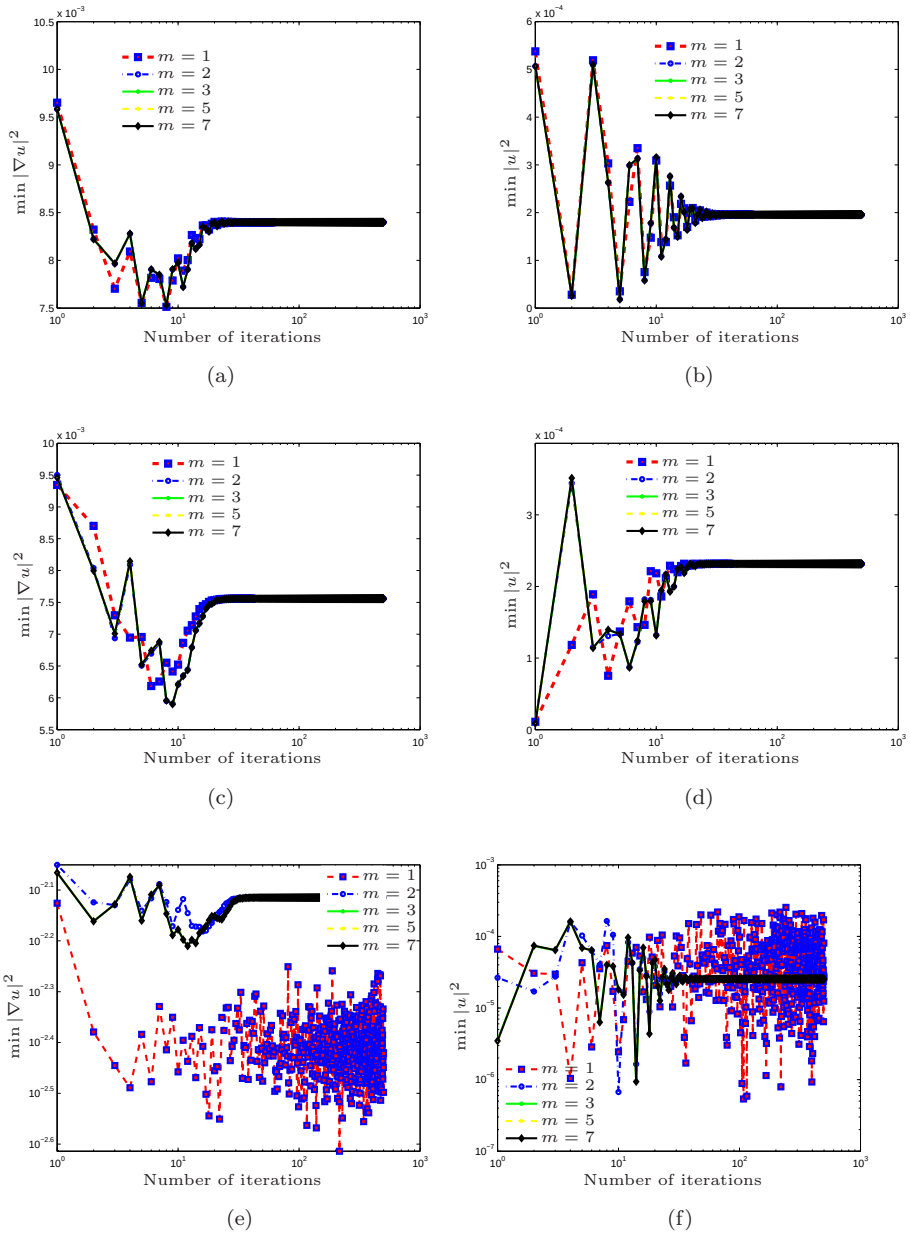

Figure 10. Plot of $\min|\nabla u|^2$ and $\min|u|^2$ versus the number of iterations for different values of $k_2 = \pi \times 10^{-m}$, where u is the numeric solution of the Helmholtz problem. (a) and (b) Case of 50 points on the boundary. (c) and (d) Case of 100 points on the boundary. (e) and (f) Case of 200 points on the boundary.

Appendix A. Proof of Lemma 1.1

Let $D(x) = F(u)f(xa) + G(u)(bx - 1)$, where $a = \frac{\tilde{\gamma}}{\gamma}$ with $b = \frac{\tilde{q}}{q}$ are unknown and $f(x) = \frac{(x-1)^2}{x+1}$. Using the linearity of the second term, and by introducing $N(x) = F(u)f(xa) - D(x)$, we see that

$$N(x) = \frac{N(x_2) - N(x_1)}{x_2 - x_1}x + \frac{x_2N(x_1) - x_1N(x_2)}{x_2 - x_1}$$
$$= \frac{N(x_1)(x_2 - x) + N(x_2)(x - x_1)}{x_2 - x_1}.$$

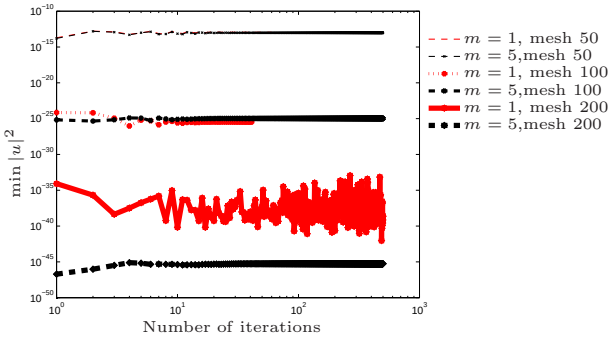

Figure 11. Plot of $\min |u|^2$ versus the number of iterations for different values of $k_1 = \pi \times 10^m$, $m = 1, 5$, where u is the numeric solution of the Helmholtz problem.

By returning to D, and by introducing the function

$$d(x_1, x_2, x) = D(x) - \frac{D(x_1)(x_2 - x) + D(x_2)(x - x_1)}{x_2 - x_1}$$

we have

$$d(_1, x_2, x) = F(u)\left[f(xa) - \frac{f(ax_1)(x_2 - x_1) + f(ax_2)(x - x_1)}{x_2 - x_1}\right],$$

which is also

$$d(x_1, x_2, x) = F(u)\left[4a^2 \frac{x(x - x_1 - x_2) + x_1 x_2}{a^3 x x_1 x_2 + a^2(x(x_1 + x_2) + x_1 x_2) + a(x_1 + x_2 + x) + 1}\right].$$

Let us define

$$Q(x_1, x_2, x_3, a) = 4a^2 \frac{x_3(x_3 - x_1 - x_2) + x_1 x_2}{a^3 x_3 x_1 x_2 + a^2(x_3(x_1 + x_2) + x_1 x_2) + a(x_1 + x_2 + x_3) + 1}.$$

We have obtained

$$d(x_i, x_j, x_k) = F(u) Q(x_i, x_j, x_k, a).$$

Note that $Q(x_i, x_j, x_k, a) = Q(x_j, x_i, x_k, a)$, but other permutation do not in general yield the same values.

As a consequence, from n distinct measurements, we obtain $3C_n^3$ identities, that is, $3C_n^3$ formulas of the form

$$\frac{1}{F(u)} = Q(x_i, x_j, x_k, a) \frac{1}{d(x_i, x_j, x_k)}. \tag{A1}$$

The value of a can thus be deducted by intersection.

Note that Q, as a function of a, has only two roots equal to zero (for $x_3(x_3 - x_1 - x_2) + x_1 x_2 \neq 0$). By an appropriate choice of x_i, x_j, x_k, we can set $a \in (0, \infty)$.

We see that the equation becomes

$$Q(x_i, x_j, x_k, a) = \frac{d(x_i, x_j, x_k)}{d(x'_1, x'_j, x'_k)} Q(x'_1, x'_j, x'_k, a).$$

Provided that the function $a \mapsto \frac{Q(x_i,x_j,x_k,a)}{Q(x'_i,x'_j,x'_k,a)}$ is bijective, a is determined uniquely. By using relation (A1), this defines F, and therefore N and finally G.

Consequently, to determine a and b, it is sufficient to choose four different points x_1, x_2, x_3 and x_4 to obtain a bijective function on $(0,\infty)$ of the form

$$a \mapsto \frac{Q(x_1,x_2,x_3,a)}{Q(x_1,x_2,x_4,a)}.$$

References

[1] *H. Ammari, E. Bonnetier, Y. Capdeboscq, M. Tanter, and M. Fink,* Electrical Impedance Tomography by Elastic Deformation SIAM J. Appl. Math. , 68(6), (2008), 1557–1573.

[2] *H. Ammari, H.Kang* Layer Potential Techniques in Imaging.Mathematical Surveys and Monographs, 153, Am. Math. Soc., Providence, 2009.

[3] *Y. Capdeboscq and M. Vogelius,* A general representation formula for boundary voltage perturbations caused by internal conductivity inhomogeneities of low volume fraction. Math. Modeling Num. Anal., 37 (2003), 159-173.

[4] *Y. Capdeboscq,* Private Communication. 2008.

[5] *H. Ammari,Y. Capdeboscq, A. Rozanova-Pierrat,* Microwave imaging by elastic perturbations. in preparation.

[6] *F. Hecht, O.Pironneau, K. Ohtsuka, A. Le Hyaric,* FreeFem++, http:// www.freefem.org/ (2007).

[7] *H. Ammari, Y. Capdeboscq, H. Kang, A. Kozhemyak* Mathematical models and reconstruction methods in magneto-acoustic imaging. Preprint.